Astron. Astrophys. 363, 1177–1185 (2000)

ASTRONOMY
AND
ASTROPHYSICS

Stark width and shift measurements of visible Si III lines

V.R. González, J.A. Aparicio, J.A. del Val⋆, and S. Mar

Universidad de Valladolid, Facultad de Ciencias, Departamento de Optica y Física Aplicada, 47071 Valladolid, Spain (victorg@opt.uva.es)

Received 12 July 2000 / Accepted 21 August 2000

Abstract. A set of experimental Stark width and shift parameters of visible doubly ionized silicon spectral lines is reported in this paper. Measurements have been made on a pulsed plasma generated in a linear discharge lamp filled with a mixture of silane and helium. Electron density and temperature in this plasma range from 0.2 to 0.9×10^{23} m^{-3} and from 17 500 to 21 000 K respectively. Electron density has been simultaneously determined by two-wavelength interferometry and from Stark broadening of He I 501.6 nm, He I 728.1 nm and H_α lines. Temperature has been simultaneously determined from Boltzmann-plot of He I lines, from absolute emission of He I lines, from Boltzmann-plot of Si II lines and from Si III/Si II intensities ratio. Dependencies of measured Stark parameters with electron density and temperature have been investigated and the final results have been compared with most of the previous experimental data as well as with some theoretical models.

Key words: atomic data – atomic processes – line: profiles – plasmas

1. Introduction

The ionized silicon spectrum is of considerable interest from the point of view of both stellar and laboratory plasma studies. In atmospheres of A, B and O type stars, and white dwarfs, a large number of ion lines has been observed (Peytremann 1972). In atmospheres of such stars, Stark broadening is the dominant pressure broadening mechanism and the knowledge of the Stark parameters in several ionization stages is very important for a number of astrophysical problems. Even in atmospheres of relative cool stars as the Sun, where line broadening caused by collisions with neutral perturbers is dominant, Stark broadening may compete with other broadening mechanisms in the line wings (Vince et al. 1985). Stark broadening of spectral lines has also regained interest for Astrophysics (Seaton 1987) with the development of researches on the physics of stellar interiors: in subphotospheric envelopes, the modellisation of energy transport requires the knowledge of radiative opacities and thus the relevant atomic process must be known with accuracy. At these high temperatures and densities the Stark broadening of multicharged ionic lines plays a non-negligible role in the calculations of the opacities.

Contrary to the case of singly ionized silicon, there are few Stark experimental data available for Si III. Therefore, it is important to provide new measurements, specially for the multiplets more sensitive to this effect. As the final result of this work, Stark width and shift of twelve visible Si III lines are given; for two of them previous experimental data did not exist.

All the results have been obtained from measurements performed in a linear discharge lamp, where a mixture of silane and helium has been purposely prepared so that self-absorption effects were minimum. This plasma source makes it possible to acquire a wide range of electron density and temperature values in a single discharge. This is particularly interesting for making calibrations of the Stark widths and shifts and will make possible other plasma diagnostics in the future.

Interferometric and spectroscopic measurements have been used to determine the electron density evolution curve, which ranges from 0.2 to 0.9×10^{23} m^{-3}. The temperature, which ranges from 17 500 to 21 000 K, has been determined from Si III/Si II intensities ratio, the Boltzmann-plot of Si II and He I lines and from absolute emission intensity measurements of He I lines. Other broadening mechanisms such as Doppler broadening or the instrumental function have been also taken into account to obtain the Stark widths. A two-temperature (2-T) partial local thermodynamic equilibrium (pLTE) model has described the plasma. Different plots of the Stark coefficients with plasma parameters have resulted in values referred to an electron density of 10^{23} m^{-3}. These values have been compared with previously published data.

2. Experimental set-up

All measurements in this work have been made in a pulsed low-pressure discharge lamp that belongs to the experimental set-up depicted in Fig. 1. All information about the excitation unit that generates the discharge and its synchronization with the detection systems is provided by Gigosos et al. (1994). We will only present here the most significant general information and the additional specific details concerning this experiment.

Send offprint requests to: S. Mar

⋆ Permanent address: Universidad de Salamanca, Departamento de Física Aplicada, E. Politécnica Superior, 05071 Avila, Spain

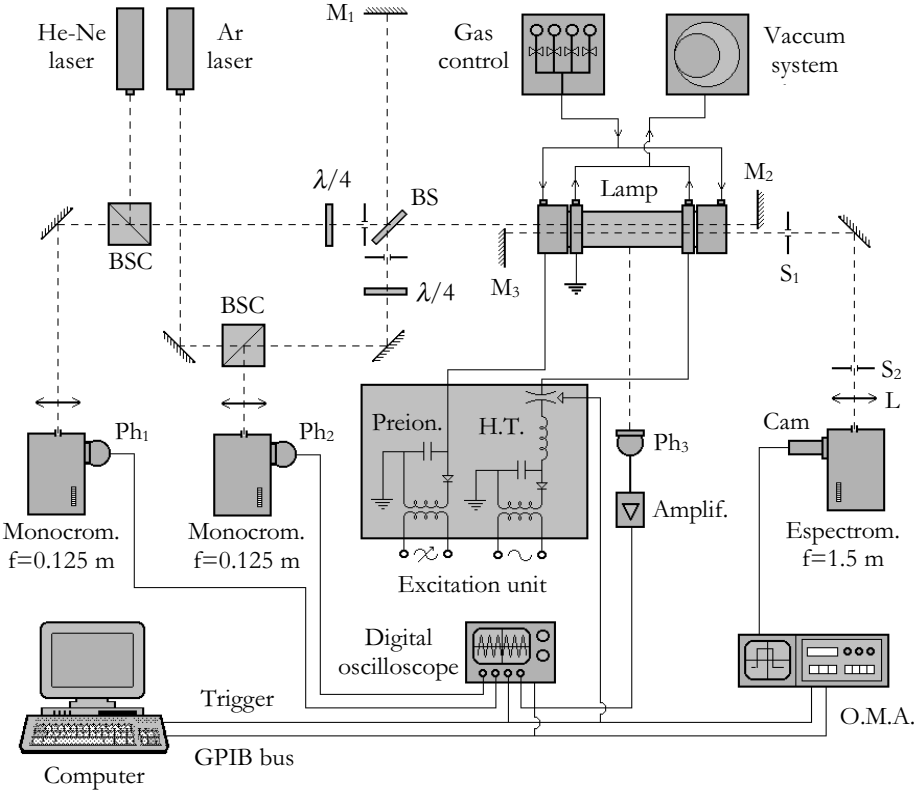

Fig. 1. Experimental arrangement.

The plasma has been generated by discharging a capacitor bank of 20 μF, charged up to 8.5 kV, on the electrodes of the lamp filled with a continuous laminar flow of a He+SiH_4 mixture. The global pressure has been 1.63×10^3 Pa at a helium rate of 11.5 ml min^{-1} and a silane rate of 0.075 ml min^{-1}. The lamp consists essentially of a cylindrical Pyrex tube (150 mm long and 18 mm of inner diameter) which ends on two annular electrodes closed by two corresponding optical windows. Silicon evaporation from tube walls and from windows has not been detected.

The basic lamp constitution, described in detail by del Val et al. (1998), has been customized for this work to account for the particular features of the plasmogen gas. Contrary to working gases of other elements, silane plasma produces a great amount of waste (not only electrode sputtering) on very few discharges, even though its concentration in the gas mixture is low and the vacuum conditions in the system are well cared for. To minimize the effect of waste on the lamp windows we have designed a protecting chamber system put before each window. Each 30 mm long chamber, which is electrically isolated from the close electrode, has a complex internal structure that limits the amount of waste that reaches the window and projects a very narrow shielding gas curtain on its inner surface. The gas feeding of the lamp has been symmetrically carried out through both chamber mouthpieces and the gas exit through the electrode ones. With respect to the transmittance of the windows the protecting chamber system extends the experiment duration from tens to hundreds of discharges. Longitudinal pressure gradients have not been detected in this 210 mm long lamp and careful measurements reveal that it preserves a high axial homogeneity and a very good cylindrical symmetry of electron density and temperature. An extensive description of this system is given by González (1999).

The gas in the lamp has been continuously preionized between consecutive plasma pulses in order to assure the good repetitiveness of discharges. To minimize the appearance of waste due to silane not the whole gas has been preionized but only a local region in the vicinity of the lamp cathode. A new electrode has been located in the protecting chamber next to the cathode to get the local preionization (González 1999). A variable voltage source feeds this arrangement to make possible a fine-tuning of the current level that ionizes the gas without unnecessary waste production. The local preionization voltage used in this work has been 500 V. Temperature and pressure of the plasma precursor gas stay well known with this kind of preionization, and it is therefore possible to make an accurate determination of the initial particle density in the lamp.

Interferometric and spectroscopic end-on measurements have been simultaneously performed all over the plasma life on two parallel plasma columns of 3-mm diameter defined by pinholes depicted in Fig. 1. Both columns are placed 2 mm off the lamp axis and in symmetrical positions referred to it. The lamp is placed in one of the arms of a Twyman-Green interferometer simultaneously illuminated by a He-Ne (632.8 nm) and an Ar^+ laser (488.0 nm). In one simply discharge is therefore possible to obtain the whole plasma refractivity changes due to only free electrons and, from them, the electron density temporal evolution. The spectra have been obtained by using a 1.5 m fo-

cal length Jobin-Yvon monochromator with a 1200 lines mm^{-1} holographic reflection grating, equipped with an optical multichannel analyser (OMA) and a 512 channel detector (EG&G 1455R-512-HQ). Mirror M_3 in Fig. 1 is employed to detect self-absorption and to reconstruct the unabsorbed spectral profiles (González 1999) if necessary.

Careful relative and absolute intensity calibrations of the spectroscopic system in the first and second diffraction orders have been performed; exhaustive details are presented by González (1999). The first one provides a transmittance function with an uncertainty around 4% and it has been employed in temperature calculations by means of the Boltzmann-plot methods. The second one supplies a calibration function with an uncertainty about 10% which has been used in temperature determination via absolute emission intensity measurement method. A wavelength calibration of the spectrometer provides the dispersion for any wavelength and diffraction order with an uncertainty lower than 1%. The inverse linear dispersion at $\lambda = 550$ nm results 12.73 pm channel^{-1} in the first order of diffraction and 4.91 pm channel^{-1} in the second order.

3. Measurements

The gas flux and the lamp pressure cited above have been purposely selected to minimize self-absorption with adequate line broadening and light levels. All the spectral lines have been registered in the first and second diffraction orders. Measurements in first order, the one with the best efficiency, have been used for temperature determination, while those at second order have been employed to obtain Stark parameters due to its highest dispersion.

For every spectral line, 11 different instants of the plasma life have been recorded, between $t = 10$ μs and $t = 110$ μs, when Si III emission decreases substantially. For each instant considered ten runs have been made, five with mirror M_3 and five without it, the exposure times usually being 5 μs. A sufficient time gap between two consecutive discharges has been selected to clean the waste in the lamp by means of the vacuum system. Nevertheless, a maximum of about 250 discharges has been performed in each single measurement session. Therefore, the evaporation of waste deposited on the lamp walls do not appreciably contribute again to the silicon plasma concentration. A total of 15 experiments with the same prefixed physical magnitudes have been made to complete all measurements. A real time check of plasma electron density and temperature repetitiveness between sessions has been performed during each experiment by periodical monitoring of width and peak intensity of the He I 667.8 nm line. Exhaustive cleaning and vacuum of the gas installation, window and tube replacement and lamp realignment have been achieved after each measurement session.

Interferometric registers of 500 μs long have been simultaneously performed with spectroscopic records to determine electron density evolution.

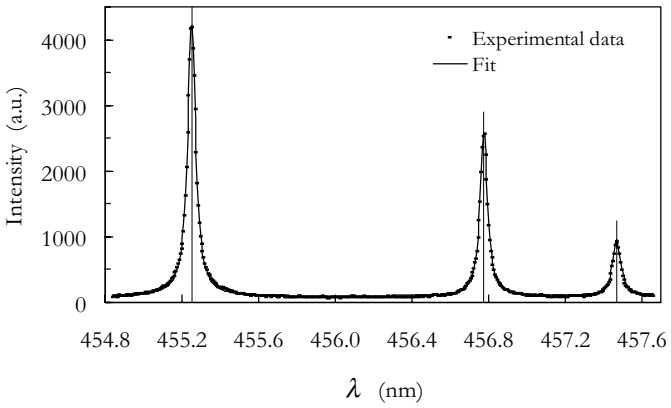

Fig. 2. An experimental spectrum of the Si III 455.3–457.5 nm lines with its corresponding fit to Eq. (1) at the instant $t = 30$ μs of the plasma lifetime.

4. Plasma diagnostics

4.1. Spectra processing

Firstly, an average of the five records taken with retro-reflection in mirror M_3, as well as an average of the five records taken without this mirror, has been made for each spectral interval registered and for each instant of the plasma life. The individual records differ from the corresponding average less than 5%, which indicates the good repeatability of this plasma source. The comparison of both averages by using the algorithms described by González (1999) gives a measurement of the plasma optical depth and therefore determines the self-absorption of each spectral line. Most of lines present no self-absorption or a value less than 15% in the peak intensity. With the mentioned algorithms is possible to obtain in a reliable way the unabsorbed emission profile in all cases.

After dividing the records by the transmittance functions of the spectroscopic channel, every spectra have been fitted to a sum of asymmetric Lorentzian functions plus a luminous background with linear dependence (Gigosos et al. 1994):

$$S(\lambda) = b_0 + b_1\lambda + \sum_{k=1}^{n} \frac{i_k + a_k\left(\lambda - \lambda_{0k}\right)/\gamma_k}{1 + \left(\lambda - \lambda_{0k}\right)^2/\gamma_k^2} \qquad (1)$$

This fitting algorithm, valid since the Stark broadening component dominates over the rest, determines the central wavelength λ_0, the peak intensity i, the asymmetry a and the full width at half maximum $\omega = 2\gamma\left[1 + (a/i)^2\right]^{1/2}$ (FWHM), of each line profile. Deviations of the fitted spectrum relative to the experimental one are less or about 2% (see Fig. 2). Asymmetries remain below 5%, which suggest that the ionic contribution to the Stark broadening of Si III lines in this plasma is not relevant.

Other broadening mechanisms like instrumental function and Doppler have also been considered when obtaining the Stark width, ω_S, from ω. Instrumental broadening has been estimated by introducing 632.8-nm laser radiation into the spectrometer and checking the FWHM of the entrance slit image. The result has been $\omega_I = 2.8$ OMA channels for the two orders of

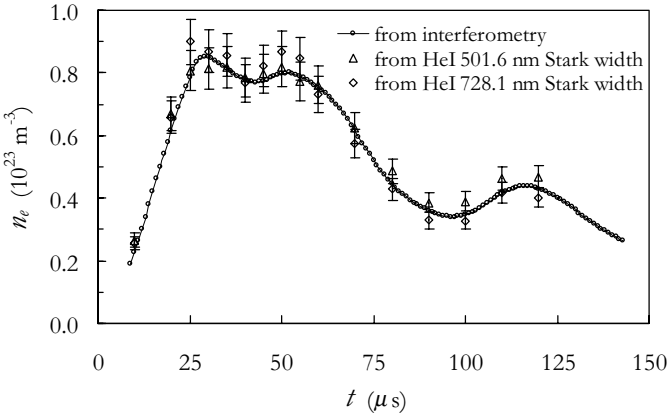

Fig. 3. Comparison between interferometric electron density curve and spectroscopic one determined by Stark broadening of two He I lines.

diffraction. Doppler width, ω_D, has been calculated by assuming a kinetic temperature for emitters around 19 000 K. As an example, Doppler width results $\omega_D = 27.1$ pm for helium and $\omega_D = 10.2$ pm for silicon when $\lambda = 550$ nm. At this wavelength, instrumental width is $\omega_I = 35.6$ pm in the first and $\omega_I = 13.7$ pm in the second order of diffraction. Every fitted spectral line has been treated like a Voigt profile, and the Stark width has been extracted from ω by using a deconvolution procedure (Davies & Vaughan 1963) represented by the polynomic expression:

$$\frac{\omega_S}{\omega} = 0.9999705 + 0.0029296x - 1.1026020x^2 + \\ + 0.0701624x^3 + 0.0296077x^4, \quad (2)$$

where $x = \omega_G/\omega$ is the fractional Gaussian line width and the Gaussian component of ω has been calculated as $\omega_G = (\omega_D^2 + \omega_I^2)^{1/2}$.

Finally, Stark shift parameters, d_S, have been directly determined from each line central wavelength value, λ_0, obtained from relation (1).

4.2. Electron density

Electron density, n_e, has been determined by two-wavelength interferometry from the plasma refractivity changes due to free electrons only, because bound electron refractivity changes do not depend on the wavelength, at least for the 476–633 nm interval (de la Rosa et al. 1990).

The phase change evolution curve $\Delta\psi_\lambda(t)$ has been obtained from every measured interferogram at each wavelength from very simple algorithms (Aparicio et al. 1998), and one average curve has been computed from tens of interferograms recorded at each experiment. This curve takes into account the whole plasma refractivity changes from $t = 0$ μs, the beginning of the discharge, to $t = 500$ μs, when the plasma is off. Mechanical vibrations are completely negligible in this temporal interval. The electron density evolution has been subsequently calculated from:

$$n_e(t) = \frac{4\pi\varepsilon_0 m_e c^2}{q_e^2}\frac{1}{2L}\frac{\lambda_2\Delta\psi_{\lambda_1}(t) - \lambda_1\Delta\psi_{\lambda_2}(t)}{\lambda_1^2 - \lambda_2^2} \quad (3)$$

In Eq. (3) L represents the plasma column length, which has been assumed to be the lamp length, 210 mm. When comparing the $n_e(t)$ curves measured at different experiments the standard deviation results lower than 5%, and therefore no significant departures have taken place. Nevertheless, each Stark width has been compared with the electron density curve measured in the corresponding experiment.

A complementary spectroscopic determination of n_e has been obtained from the Stark broadening of the 501.6 nm and 728.1 nm He I lines. Previous calibrations presented in Eqs. (5), performed in this laboratory with an analogous plasma source (Pérez et al. 1991, 1995), electron densities between 10^{22} and 1.5×10^{23} m^{-3} and temperatures around 20 000 K, have been used:

$$\ln\omega_{S,\mathrm{He\,I}\,501.6}[\mathrm{pm}] = -(49.3 \pm 1.8) + \\ + (1.08 \pm 0.02)\ln n_e[\mathrm{m}^{-3}] \\ - (0.12 \pm 0.04)\ln T[\mathrm{K}] \quad (4)$$

$$\omega_{S,\mathrm{He\,I}\,728.1}[\mathrm{pm}] = (28 \pm 11) + \\ + (896 \pm 14) \times 10^{23} n_e[\mathrm{m}^{-3}] \quad (5)$$

These lines emit strongly and have a notable Stark width in the experimental conditions of this work. Also, they are almost very insensitive to the ion dynamics effects (Mijatovic et al. 1995) and so their Stark profiles correspond to the pure electron impact. The interferometric and He I Stark width-based diagnostics of electron density are compared in Fig. 3. The curves in the figure follow the temporal shape of the high current pulse applied on the lamp closely, and this picture shows the good agreement between the interferometric and spectroscopic determinations of $n_e(t)$.

The electron density has also been obtained by measuring the temporal evolution of the H_α Stark broadening, which is achievable due to the small amount of hydrogen present in silane. The He I and the H_α profile records have been inserted between the Si III ones and have been performed with 3 μs exposures. They have been corrected from self-absorption, the maximum value being 10% for He I lines and 15% for H_α line, and the Stark width of He I profiles has been obtained as described in the previous paragraph. However, with the experimental conditions of this work, the H_α line is sensitive to ion dynamics effects (Gigosos & Cardeñoso 1987) and it does not present a pure electron impact profile. Consequently, its Stark width can not be obtained from a simple deconvolution procedure and the FWHM does not define the electron density completely. It is possible to make an electron density diagnostic by comparing the H_α FWHM from the measured profiles and those calculated by simulation techniques developed in this laboratory (Gigosos & Cardeñoso 1987, 1996) based on the μ-ion model. The reduced mass corresponding to the plasma of this work is $\mu = 0.8$ since hydrogen emitters are almost completely rounded by helium

perturbers. The interferometric and H_α Stark FWHM-based diagnostics of electron density are compared in Fig. 4. A very good agreement between interferometric and spectroscopic H_α determinations of $n_e(t)$ exists from $t = 40$ μs on. However, in the earliest instants of the plasma life the calculated profile widths corresponding to interferometric-based values of electron density are greater than measured ones. Therefore, the electron density seems to be notably smaller than that predicted by the interferometric diagnostic. Taking into account the previous good results illustrated in Fig. 3 it may be possible to reject this possibility. A reasonable explanation for this effect can be obtained assuming that ionic kinetic temperature is lower than the electronic one (González 1999). Comparison of the experimental H_α profile shapes with those calculated taking into account this hypothesis, which can be achieved in a equivalent scheme where the ions have a reduced mass greater than $\mu = 0.8$, shows that ionic temperature is about 0.2 times the electron temperature ($\mu = 4.0$) until $t = 30$ μs; around this instant a rapid thermalisation process of both species begins, ending the kinetic decoupling about $t = 45$ μs. This result shows that the plasma probably has a 2-T behaviour (van der Mullen 1990) at the initial instants, when the rise flank of the high current pulse applied on the lamp "drives" the plasma. At these instants the applied external electric field heats more the electrons than ions; later, the collisionnal processes in the plasma prevail and the kinetic energy is redistributed.

The good agreement found between the independent interferometric and spectroscopic determinations of n_e(t) reinforces the assumption made for L as the lamp length and therefore the negligible influence of possible inhomogeneous boundary layers. We conclude that in this work the electron density, which ranges between 0.2 and 0.9×10^{23} m^{-3}, has been determined with uncertainties lower than 10% and from now on we will take the interferometric determination of n_e as a reference for other comparisons and calculations.

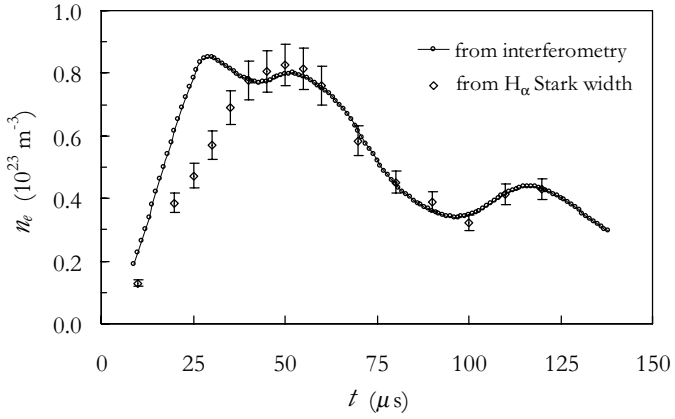

Fig. 4. Comparison between interferometric electron density curve and spectroscopic one determined by Stark FWHM of the H_α line.

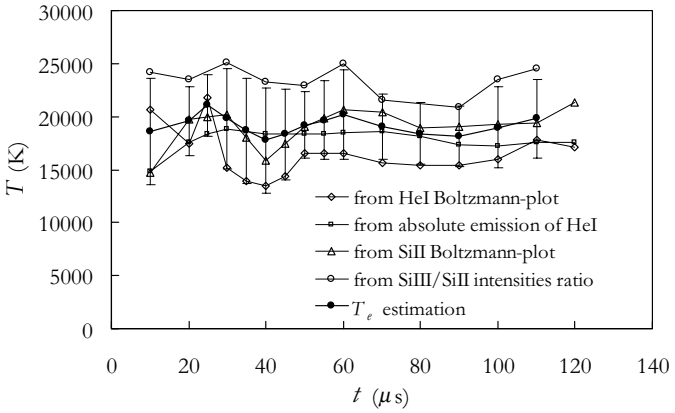

Fig. 5. Electron temperature estimation from Boltzmann-plot methods, from consecutive silicon ion intensities ratio and from absolute He I emission measurements.

4.3. Temperature

The relevant temperature parameter in Stark broadening and shift of spectral lines of multiply-charged ions is the kinetic electron temperature, T_e. It is very usual in these kinds of collision-dominated plasmas to assume that T_e is very similar to the ion excitation temperature (van der Mullen 1990). In this work the Si III excitation temperature has been calculated from the Si III/Si II intensities ratio assuming total LTE. This calculation has been performed with the multiplet (2) of Si III (λ =455.3, 456.8 and 457.5 nm lines) and the multiplet (5) of Si II (λ =504.1 and 505.6 nm lines). The silicon excitation temperature has also been calculated from a Si II Boltzmann-plot assuming pLTE. This plot involves the Si II lines of the five most prominent visible low-excitation multiplets. Their upper energy levels cover an energy interval of about 3 eV (between 10.067 and 12.839 eV). Additional determinations of T have been obtained from the absolute emission intensity measurements of He I lines, assuming total LTE, and from the He I excitation temperature by using a He I Boltzmann-plot and assuming partial LTE. The He I lines used for this calculations were 471.3, 501.6, 706.5 and 728.1 nm, whose upper energy levels cover only an energy interval of about 1 eV (between 22.719 and 23.594 eV). The statistical errors corresponding to the diverse determinations are: around 10% for Si III/Si II intensities ratio method, around 14% for Si II Boltzmann-plot method, around 18% for He I Boltzmann-plot method, and around 7% for absolute emission of He I method. The temperature curves are shown in Fig. 5. In this figure has also been depicted an average of the four previous determinations with an error band around 20%. This average curve does not have any physical meaning since the various methods to calculate the plasma temperature are not comparable in a simple way. However, this curve can be considered as a reasonable working estimation of the kinetic electron temperature, T_e. A more profound analysis of the plasma temperature is given by González (1999) but, summarizing, it can be pointed out that there is evidence that for He I the plasma has an ionizing (van der Mullen 1990) behaviour while for Si III the plasma has a recombining (van der Mullen 1990) behaviour. This fact is reflected in Fig. 5 since the excitation temperature for He I is less than T_e and the opposite occurs for Si III.

The final estimation for T_e ranges from 17 500 to 21 000 K with a statistical uncertainty of about 20%. This result is reasonably satisfactory if the high uncertainty of the Si II and Si III probability transitions (about 25%) and the small difference between the He I energy levels used in the Boltzmann-plot methods are taken into account. In this experiment there are no direct measurements available to determine the kinetic temperature of the emitters, which creates an ambiguity in relation to the estimation of the Doppler contribution to the total linewidth. The results obtained in Sect. 4.2 in relation to an ionic temperature about 0.2 times lower than the electronic one in the first instants of the plasma life, seem to indicate than Si III emitters could have a kinetic temperature of about 4000 K during these instants. Processing of line profiles with this temperature generates a discrepancy with respect to those processed with the reference temperature of 19 000 K, not higher than 10% in the narrowest Si III lines at $n_e = 10^{23}$ m^{-3}.

5. Results and conclusions

The different ω_S-values measured for every spectral line at the diverse instants of the plasma life have been divided by the corresponding n_e value and have been plotted against the measured temperature to check its influence in Stark broadening. No functional trend can clearly be distinguished from our data due to the small differences between them in comparison with the error band and the narrow range of temperatures found in our experiment. Therefore, the data have been plotted against n_e for each measured line. Very clear linear dependencies have been observed. The resulting width values at $n_e = 10^{23}$ m^{-3} have been determined from the linear fit (ω_m from now on).

In relation to shifts, since the line centre is not available at null electron density, these have been obtained from a linear extrapolation of all line centres measured for each line as a linear function of n_e. The inverse linear dispersion at the given wavelength multiplied by the difference between any line centre and that obtained from the extrapolation yields the corresponding Stark shift, d_S. We have called d_m the shift evaluated from this linear fit at $n_e = 10^{23}$ m^{-3}. As well as Stark widths, no clear functional trends of Stark shifts with temperature have been observed. One example of the plots performed for Stark parameter calibrations is shown in Fig. 6 for the Si III 455.3 nm.

The final results are listed in Table 1. As cited above, all data have been normalised at $n_e = 10^{23}$ m^{-3}. Transition array and multiplet -with its identification number (Moore 1965) specified in parenthesis when available- are indicated in the first and second columns of the table, respectively. The corresponding wavelengths are presented in the third column. The multiplets have been ordered by increasing average wavelength and the spectral lines in a multiplet have been ordered by decreasing lower and upper quantum numbers. The measured ω_m and d_m values are indicated in picometers in columns four and five, respectively. The Stark parameters obtained in this work (column six of the tables) are accompanied by their statistical error calculated as $\sigma(a_\omega) + 10^{23}\sigma(b_\omega)$, where $\sigma(a_\omega)$ and $\sigma(b_\omega)$ are the statistical error of the coefficients in the linear fitting $\omega_m = a_\omega + b_\omega n_e$.

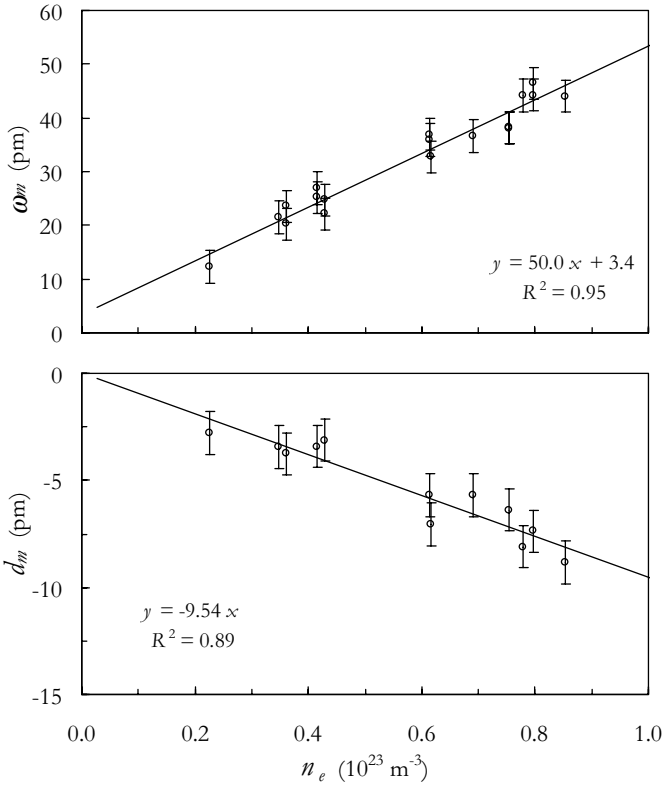

Fig. 6. Stark width and shift calibrations for the Si III 455.3 nm line. R^2 is the linear correlation coefficient for the fit of the data.

This way to compute the error usually overestimates its final level though it takes into account both the intrinsic quality of the fit and other errors which may be produced by a small but non-null a_ω value. Data from previous experimental works (Puric et al. 1974; Platisa et al. 1977; Kusch & Schröder 1982; Djenize et al. 1992) are also listed in columns four and five. The plasma electron density and temperature conditions involved in each experiment are presented in Table 2. When the reviewers have evaluated the uncertainty for these data, it appears just next to the values in columns four and five of Table 1 as the usual qualified letter. In these columns we also give the Stark FWHM values obtained on the basis of various theoretical calculations. Label "th. G" in column six stands for the theoretical results calculated by Dimitrijevic & Konjevic (1980, 1981) by the semi-classical formula of Griem (1974). Labels "th. SE" and "th. ASC" denote results obtained by Dimitrijevic & Konjevic (1980, 1981) and by Dimitrijevic (1983), on the basis of the semi-empirical calculations according to Griem (1974), and of the approximative semi-classical calculations, respectively. Finally, label "th. MSE" denotes results calculated on the basis of modified semi-empirical approach by Dimitrijevic & Konjevic (1980, 1981, 1987) and by Dimitrijevic (1983, 1988). The temperature range for the theoretical values presented in the table is 10 000–30 000 K.

Stark linewidth data for multiplets (2), (4) and (5) are shown in Fig. 7. This work data have been represented with their error bars at the edges and at the middle point of the measured tem-

Table 1. Stark width and shifts for the Si III lines measured in this work compared with results from previous experimental and theoretical works. Next to each measured value its statistical error as a percentage is indicated, or the qualified letter assigned by reviewers. All values are referred to $n_e = 10^{23}$ m^{-3} except those of Platisa et al. (1977) ($n_e = 0.58 \times 10^{23}$ m^{-3}).

Transition	Multiplet (No)	λ (nm)	ω_m (pm)	d_m (pm)	Reference
$4p - 4d$	$^3P^O - ^3D$ (5)	380.653	$69 \pm 24\%$	$42 \pm 23\%$	This work
			47 D+		Kusch & Schröder (1982)
			45.5–58.4		Djenize et al. (1992)
			106–69.1		th. G
			74.6–52.9		th. ASC
			45.6–33.8		th. SE
			76.2–46.3		th. MSE
		379.612	$68 \pm 22\%$	$43 \pm 22\%$	This work
			48 D+		Kusch & Schröder (1982)
			106–69.1		th. G
			74.6–52.9		th. ASC
			45.6–33.8		th. SE
			76.2–46.3		th. MSE
		379.140	$68 \pm 27\%$	$39 \pm 28\%$	This work
			20.4 C+		Platisa et al. (1977)
			37 D+		Kusch & Schröder (1982)
			106–69.1		th. G
			74.6–52.9		th. ASC
			45.6–33.8		th. SE
			76.2–46.3		th. MSE
$4s - 4p$	$^3S - ^3P^O$ (2)	455.262	$53 \pm 8\%$	$-10 \pm 11\%$	This work
			48–38 C	5–5 C	Puric et al. (1974)
			18 C+		Platisa et al. (1977)
			93.2–59.4		th. G
			60.4–42.2		th. ASC
			43.8–25.3		th. SE
			72.8–42.0		th. MSE
		456.784	$50 \pm 9\%$	$-8 \pm 19\%$	This work
			56–67 C	4–7 C	Puric et al. (1974)
			58 C+		Platisa et al. (1977)
			93.2–59.4		th. G
			60.4–42.2		th. ASC
			43.8–25.3		th. SE
			72.8–42.0		th. MSE
		457.476	$50 \pm 10\%$	$-9 \pm 22\%$	This work
			17.6 C+		Platisa et al. (1977)
			306 [a] D		Kusch & Schröder (1982)
			93.2–59.4		th. G
			60.4–42.2		th. ASC
			43.8–25.3		th. SE
			72.8–42.0		th. MSE
$4f - 5g$	$^3F^O - ^3G$ (9)	481.333	$398 \pm 38\%$	$-98 \pm 55\%$	This work
			292		Djenize et al. (1992)
		481.971	$425 \pm 30\%$	$-98 \pm 55\%$	This work
			292		Djenize et al. (1992)
		482.896	$405 \pm 15\%$	$-98 \pm 55\%$	This work
			307		Djenize et al. (1992)
$4s - 4p$	$^1S - ^1P^O$ (4)	573.973	$87 \pm 21\%$	$-16 \pm 35\%$	This work
			71 D+		Kusch & Schröder (1982)
			159–102		th. G
			102–72.9		th. ASC
			73.6–46.8		th. SE
			125–72.4		th. MSE
$4d - 5p$	$^3D - ^3P^O$	746.599	$647 \pm 32\%$		This work
		746.250	$520 \pm 51\%$		This work

[a] A misprint or arithmetical error is likely in the value presented by the authors.

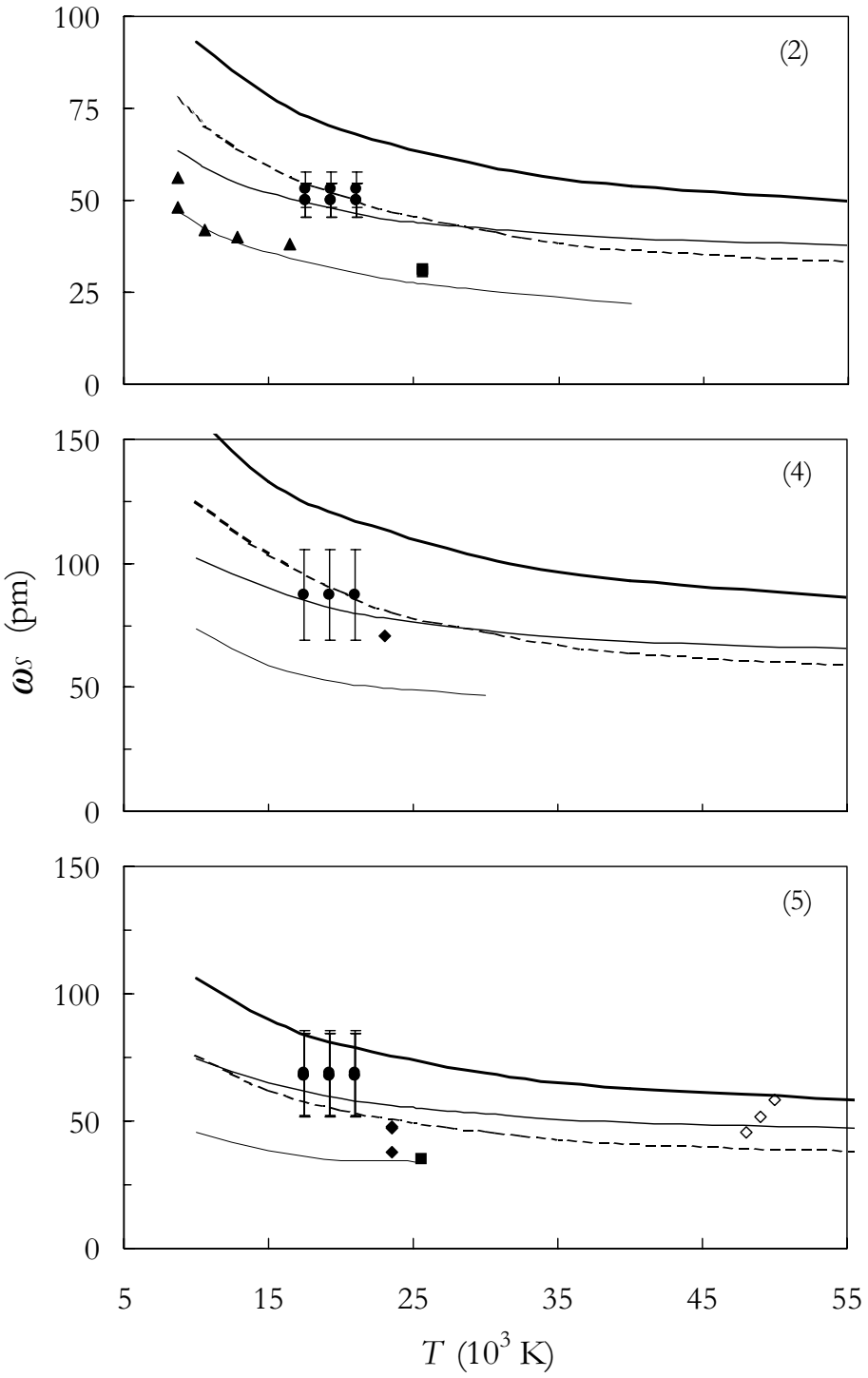

Fig. 7. Stark FWHM at $n_e = 10^{23}$ m^{-3} versus temperature for the Si III multiplets (2), (4) and (5) measured in this work (●). Results are compared with previous measurements: ▲ (Puric et al. 1974), ■ (Platisa et al. 1977), ♦ (Kusch & Schröder 1982) and ◇ (Djenize et al. 1992), and with theoretical predictions: —— G (Dimitrijevic & Konjevic 1980, 1981), —— ASC and —— SE (Dimitrijevic and Konjevic 1980, 1981; Dimitrijevic 1983) and - - - MSE (Dimitrijevic & Konjevic 1980, 1981, 1987; Dimitrijevic 1983, 1988).

perature interval. For the multiplet (2) – $\lambda = 455.3$, 456.8 and 457.5 nm – the values measured in this work are higher than those from Puric et al. (1974) and Platisa et al. (1977), which are in a good agreement with SE model. Values from this work are, however, in a close agreement with ASC and MSE models, and this is also true for multiplets (4) – $\lambda = 573.97$ nm – and (5) – $\lambda = 380.7$, 379.6 and 379.1 nm –. Values calculated with both models are very similar from $T = 15\,000$ K on, but the MSE model predicts a more pronounced decrease of Stark broadening with temperature. It is difficult to distinguish the model which fits better the experimental values, but multiplet (5) data from the present work and from Djenize et al. (1992) seem to indicate a better fit is produced by ASC model. Data from Kusch & Schröder (1982) also show a good agreement with this work and with ASC and MSE models in multiplet (4), although the data for multiplet (5) are approximately equidistant between these models and SE model. On the other hand, values predicted for the semi-classical G model are systematically higher than those

Table 2. Summary of electron density and temperature ranges concerning the experiments considered for comparisons with this work.

Reference	n_e (10^{23} m^{-3})	T (10^4 K)
This work	0.2–0.9	1.75–2.10
Puric et al. (1974)	2.95–5.6	0.87–1.64
Platisa et al. (1977)	0.58	2.56
Kusch & Schröder (1982)	0.5–2.0	2.25–2.50
Djenize et al. (1992)	1.4–2.6	4.80–5.00

measured in this work, although the differences decrease when the multiplet number increases (and also the upper level energy of the transition).

For multiplet (9) – $\lambda = 481.3$, 482.0 and 482.9 nm –, which is among the most sensitive to the Stark effect, the measured FWHM in this work is about 400 pm at $n_e = 10^{23}$ m^{-3}, whereas that measured by Djenize et al. (1992) is about 300 pm. To compare these data it is necessary to account for the temperature difference between both experiments (about 30 000 K). Such a discrepancy in the linewidth values is reasonable under the assumption of a decrease with T similar to that corresponding to multiplets (2), (4) and (5). For multiplet $^3D - ^3P^O$ – $\lambda = 746.3$ and 746.3 nm –, the most sensitive to the Stark effect, there exists no previous experimental data with which to compare. Theoretical calculations for both multiplets have not been found in the literature.

In relation to the Stark shift, one previous work provides experimental values for only two lines. Puric et al. (1974) give for multiplet (2) a blue shift $d_m = 4$–7 nm whereas in this work a red shift $d_m = (-8)$–(-10) nm has been measured. Shift calculations are not available in the literature.

As a final conclusion, Stark width and shifts of several interesting Si III multiplets have been measured in this work. Although the temperature range is not wide enough to discriminate clearly between theories, results obtained are in good agreement with the approximative semi-classical calculations (ASC) of Dimitrijevic and Konjevic. This work offers probably the most extensive experimental compilation of Si III Stark widths and shifts in the visible performed up to now.

Acknowledgements. The authors thank doctors M.A. Gigosos, C. Pérez and M.I. de la Rosa for their valuable suggestions and comments, S. González for his collaboration in the experimental arrangement, and the Spanish Dirección General de Investigación Científica y Técnica (Ministerio de Educación y Ciencia) and the Consejería de Educación y Cultura de Castilla y León for their financial support under contracts No. PB98-0356 and VA23-99 respectively. Dr. J.A. Aparicio wants to express his personal acknowledgement to the Organización Nacional de Ciegos de España (ONCE) for his help.

References

Aparicio J.A., Gigosos M.A., González V.R., et al., 1998, J. Phys. B 31, 1029
Davies J.T., Vaughan J.M., 1963, ApJ 4, 1302
Dimitrijevic M.S., 1983, A&A 127, 68
Dimitrijevic M.S., 1988, A&AS 76, 53
Dimitrijevic M.S., Konjevic N., 1980, JQSRT 24, 451
Dimitrijevic M.S., Konjevic N., 1981, In: Wende B. (eds.) Spectral Line Shapes. W. de Gruyter, Berlin, New York, p. 211
Dimitrijevic M.S., Konjevic N., 1987, A&A 24, 451
Djenize S., Sreckovic A., Labat J., Puric J., Platisa M., 1992, J. Phys. B 25, 785
Gigosos M.A., Cardeñoso V., 1987, J. Phys B 20, 6006
Gigosos M.A., Cardeñoso V., 1996, J. Phys B 29, 4795
Gigosos M.A., Mar S., Pérez C., de la Rosa I., 1994, Phys. Rev. E 49, 1575
González V.R., 1999, Ph.D. Thesis, Universidad de Valladolid
Griem H.R., 1974, Spectral Line Broadening by Plasmas. Academic Press, New York
Kusch H.J., Schröder, 1982, A&A 116, 255
Mijatovic Z., Konjevic N., Ivkovic M., Kobilarov R., 1995, Phys. Rev. E 51, 4891
Moore C.E., 1965, Selected Tables of Atomic Spectra. NSRDS-NBS 3, Sect. 1.
van der Mullen J.A.M., 1990, Phys. Rep. 191, 109
Pérez C., de la Rosa M.I., de Frutos A.M., Mar S., 1991, Phys. Rev. A 44, 6785
Pérez C., de la Rosa M.I., Aparicio J.A., Gigosos M.A., Mar S., 1995, Phys. Rev. E 51, 3764
Peytremann E., 1972, A&A 17, 76
Platisa M., Dimitrijevic M., Popovic M., Konjevic N., 1977, J. Phys. B 10, 2997
Puric J., Djenize S., Labat J., Cirkovic Lj., 1974, Z. Physik 267, 71
de la Rosa M.I., Pérez C., de Frutos A.M., Mar S., 1990, Phys. Rev. A 42, 7389
Seaton M.J., 1987, J. Phys. B 20, 6363
del Val J.A., Mar S., Gigosos M.A., et al., 1998, Jpn. J. Appl. Phys. 37, 4177
Vince I., Dimitrijevic M.S., Krsljanin V., 1985, In: Rostas F. (ed.) Spectral Line Shapes III, W. de Gruyter, Berlin, New York, p. 649